RESEARCH PAPER

Experimental and numerical analyses of circular footing on geogrid-reinforced granular fill underlain by soft clay

Ahmet Demir · Abdulazim Yildiz · Mustafa Laman · Murat Ornek

Abstract Experimental and numerical investigations into the bearing capacity of circular footing on geogrid-reinforced compacted granular fill layer overlying on natural clay deposit have been conducted in this study. A total of 8 field tests were carried out using circular model rigid footing with a diameter of 0.30 m. 3D numerical analyses were performed to simulate soil behavior using finite element program Plaxis 3D Foundation. The results from the FE analysis are in very good agreement with the experimental observations. It is shown that the degree of improvement depends on thickness of granular fill layer and properties and configuration of geogrid layers. Parameters of the experimental and numerical analyses include depth of first reinforcement, vertical spacing of reinforcement layers. The results indicate that the use of geogrid-reinforced granular fill layers over natural clay soils has considerable effects on the bearing capacity and significantly reduces the lateral displacement and vertical displacement of the footing.

A. Demir
Civil Engineering Department, Osmaniye Korkut Ata
University, 80000 Osmaniye, Turkey
e-mail: ahmetdemir@osmaniye.edu.tr

A. Yildiz · M. Laman (✉)
Civil Engineering Department, Cukurova University,
01330 Balcali, Adana, Turkey
e-mail: mlaman@cukurova.edu.tr

A. Yildiz
e-mail: azim@cukurova.edu.tr

M. Ornek
Civil Engineering Department, Mustafa Kemal University,
31200 Iskenderun, Hatay, Turkey
e-mail: mornek@mku.edu.tr

1 Introduction

Soft soils, such as normally consolidated or slightly over-consolidated clays, have high compressibility and low shear strength. Construction on soft soils often requires utilization of ground improvement techniques such as soil reinforcement. Shallow foundations may be attempted for construction of structures by placing a compacted granular fill layer of limited thickness over the soft clay subsoil. Fill layer increases the load-bearing capacity of the foundation and decreases the settlement at allowable load. Recently, with the development and use of geosynthetics in civil engineering projects, it appears that the load-bearing capacity can be further increased by placing a layer of geogrid at the interface of the clay subsoil and the compacted granular fill. The beneficial effects of using geogrid reinforcement have been clearly demonstrated by several investigators. Construction of geogrid reinforcement incorporated at the base of a layer of granular fill placed on a soft clay subgrade is commonly used for unpaved roads, embankments, and large stabilized areas such as car parks or working platforms for oil drilling [9, 12, 13, 16, 24–27, 29, 33, 34]. Rowe and Soderman [33] investigated the potential effects of geotextile reinforcement upon the stability of embankments constructed on peat which is underlain by a soft clayey layer. The use of a geotextile in conjunction with lightweight fill appears to be the most satisfactory means of improving the performance of embankments on these very poor foundations. It was shown that reinforcement can significantly reduce the maximum lateral displacements, vertical displacements,

and foundation soil heave during embankment construction [34]. Fannin and Sigurdsson [9] investigated the stabilization of unpaved roads on soft ground with geosynthetics. It was shown that the combination of geosynthetic reinforcement and fill helps to spread the concentrated vertical loads and to inhibit large deformations and local failures. Geosynthetics reinforcing unpaved roads on soft subgrade have been shown to reduce the necessary fill thickness by approximately 30 % [29]. Ling and Liu [24] investigated the performance of geosynthetic-reinforced asphalt pavement under monotonic, cyclic, and dynamic loading conditions. This study showed that geosynthetic reinforcement increased the stiffness and bearing capacity of the asphalt concrete pavement. Under dynamic loading, the life of the asphalt concrete layer was prolonged in the presence of geosynthetic reinforcement. The stiffness of the geogrid and its interlocking with the asphalt concrete contributed to the restraining effect. Ling and Liu [25] describe two-dimensional finite element studies that analyzed the behavior of reinforced asphalt pavement under plane strain conditions and subject to monotonic loading. Ling and Liu [26] present a simple constitutive model for the behavior of sands during monotonic simple shear loading. The model is developed specifically to account for the effects of principal stress rotation on the simple shear response of sands.

In comparison with other applications of geosynthetic-reinforced soil, for example, geosynthetic-reinforced soil embankments, roads, or retaining walls, relatively less emphasis has been placed on reinforced soil footings. There have been many studies of shallow foundations on reinforced soil systems, most of them concentrating on sandy soil [1, 7, 8, 10, 11, 14, 19, 37].

Yamamoto et al. [37] investigated the geotechnical performance of various types of foundations on sand using model loading tests and the numerical limit analysis. A series of model loading tests, in which the ground was simulated using aluminum roads, were conducted to determine the performance of different types of foundations. The numerical limit analysis showed reasonably good agreement with the model tests for both surface and embedded foundations. The results showed that the bearing capacity of T-bar, shell block, and rigid block foundations has increased when the interface condition at the base and side of the foundation was gradually varied from smooth to rough conditions.

However, a limited number of studies are available at the present time relating to the bearing capacity of shallow foundations on reinforced granular material of limited thickness overlying soft clay [6, 17, 20, 27, 31]. Love et al. [27] studied the effectiveness of geogrid reinforcement, placed at the base of a layer of granular fill on the surface of clay by small-scale model tests in the laboratory. In the tests, only one geogrid layer was used at the interface between granular fill and clay soil. They showed that performance of reinforcement systems to be excellent even at small deformations, due to the significant change in the pattern of shear forces acting on the surface of the clay. According to the author's knowledge, when used more than one geogrid in granular fill, the effect of the geogrid-reinforced granular fill layer on the bearing capacity behavior of foundations on natural clay deposits has not yet been investigated extensively in the geotechnical engineering. This paper relates to some recent field test results which were conducted to determine the bearing capacity and settlement behavior of circular footing supported by a reinforced stiffer granular layer of limited thickness over soft clay. The problem has also been simulated by 3D numerical analysis based on the finite element method. In order to validate the approach of the numerical analysis, the results are compared with the results of field tests.

2 Field tests

The bearing capacity of circular rigid footing on geogrid-reinforced compacted granular fill layer overlying on natural clay deposit has been investigated using field tests. The parameters investigated in the tests include the depth of first reinforcement layer (u) and the location of second reinforcement layer (h). A total of 8 field tests were carried out using circular rigid footing with a diameter of 0.30 m.

2.1 Site characterization

The field tests have been conducted in the Adana Metropolitan Municipality's (AMM) Water Treatment Facility Center (WTFC) located in west part of Adana, Turkey. Two test pit excavations and four borehole drillings were performed in the experimental site. Ground water level was observed as 2.20 m from borehole drillings. The characteristics of the soil at the experimental site have been determined through an extensive testing program that consisted of a combination of laboratory and in situ tests. The site investigation revealed a 10.0-m-thick upper layer of homogeneous silty clay and following a hard calcerus layer. The clay content of the soil layers varies in the range between 60 and 70 %. The silty clay layer is classified as high plasticity clay (CH) and the water content of the stratified soil layers varies between 20 and 25 % depending on depth, and is almost the same as or greater than the plastic limit of the clay. Soil strengths were measured with a vane apparatus in test pits TP1 and TP2. Unconsolidated undrained (UU) triaxial tests were also performed on samples taken from borehole drillings at different depths. These tests gave a mean undrained shear strength of 65 kN/m^2 for purposes of the numerical analysis reported next. The silty clay is classified as slightly overconsolidated based on odometer test results.

2.2 Granular fill

The granular fill material used in the field tests was obtained from Kabasakal region situated northwest of Adana, Turkey. Granular soil was prepared at a value of optimum moisture content of 7 % and a maximum dry unit weight of 21.7 kN/m^3. The values of internal friction angle and the cohesion of granular fill were obtained as 43° and 15 kN/m^2, respectively, from direct shear tests. Specific gravity of the granular soil was obtained as 2.64. Typical soil characteristics of granular fill material are given in Fig. 1. From the sieve analysis, granular soil was classified as well-graded gravel–silty gravel, GW–GM according to the unified soil classification system. Figure 1a shows particle size distribution of natural granular fill material. However, granular fill material used in laboratory conventional and field test was obtained from natural granular material passing through 4.75-mm opening sieve. The reason was to provide homogeneity in laboratory and field test conditions.

2.3 Geogrids

A white-colored, Secugrid Q-type geogrid with a maximum tensile strength of 60 kN/m was used as reinforcing material in the field tests. The physical and mechanical properties of the geogrids as listed by the manufacturer are given in Table 1.

2.4 Experimental setup and test program

Reaction piles were constructed on the test field. Then, reaction piles were connected to each other with a steel beam. The top surface of the test area was leveled, and the rigid footing was placed on a predefined alignment such that the loads from the hydraulic jack and loading frame would be transferred concentrically to the rigid footing. A hydraulic jack against the steel beam provided downward load. Hydraulic jack and two linear variable displacement transducers (LVDT) were connected to a data logger unit, and data logger unit was connected to a computer. The granular fill material was placed and compacted in 50-mm layers. The amount of granular fill material and water needed for each layer was first calculated. Then, the granular fill material was compacted using a plate compactor to a predetermined height to achieve the desired densities. When the desired reinforcement depth was reached, geogrid layer was placed and compaction was then continued until the desired granular fill height was reached. Load was applied with a hydraulic jack and maintained manually with a hand pump until the vertical displacement, that is, settlements recorded 15 % of rigid footing diameter. The load and the corresponding rigid footing settlement were measured by a calibrated pressure gauge and two LVDTs, respectively. The testing procedure was performed according to the ASTM D 1196-93 [2], where the load increments applied and maintained until the rate of
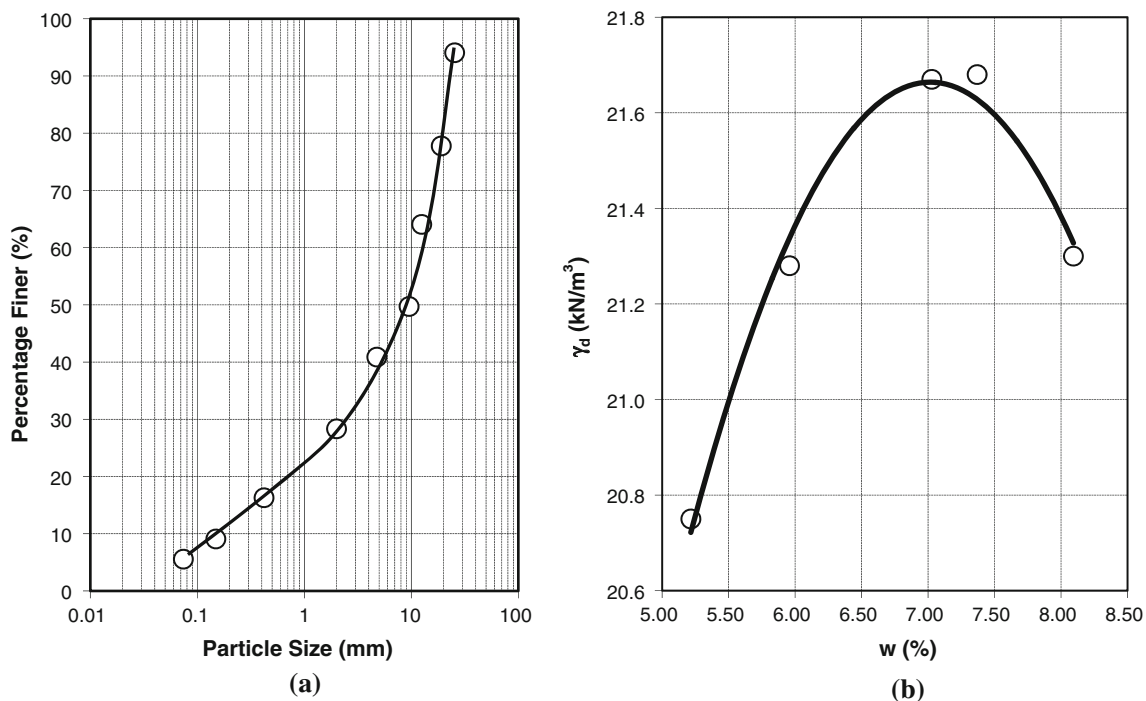

Fig. 1 Typical soil characteristics of granular fill material. **a** Particle size distribution (natural granular material), **b** optimum moisture content

Table 1 Engineering properties of geogrid

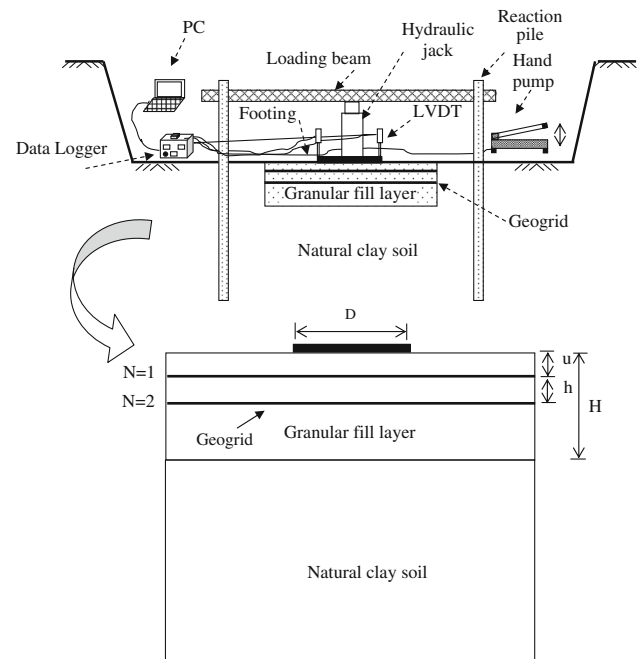| Parameters	Values
Structure	Biaxial
Aperture shape	Squared
Aperture size	31 mm $\times$ 31 mm
Mass per unit area	360 g/m^2
UV resistance	>94 %
Raw material	Polypropylene
Elongation at nominal strength	8 %
Tensile strength at 2 % elongation	22/22 (md/cmd) (kN/m)
Tensile strength at 5 % elongation	48/48 (md/cmd) (kN/m)

settlement was less than 0.03 mm/min over three consecutive minutes. To maintain the same density in the granular fill layer, the convenient compactive effort was applied on each layer of granular fill. Some tests were repeated twice to verify the repeatability and the consistency of the test data. The difference was considered to be small and neglected. After each test was completed, the granular fill layer was carefully excavated and the geogrid reinforcement visually inspected. The tests were continued until the applied vertical load was clearly reduced or a considerable settlement of the rigid footing was obtained from a relatively small increase in vertical load. Detailed information of the testing procedure can be found in Laman et al. [21, 23] and Ornek [31]. The general layout of the test setup is given in Fig. 2.

The research was initially conducted on the natural clay deposit. In reinforced case, the rigid footing was placed on geogrid-reinforced granular fill layer underlain by natural soft clay deposit. The thickness of the granular fill layers was kept constant as 0.20 m ($H = 0.67D$). The main purpose in reinforced case is to investigate the most suitable geogrid configuration parameters such as u and h that maximizes bearing capacity and minimizes settlement of the rigid footing. Firstly, the effect of first geogrid layer depth on bearing capacity of the footing was investigated for different values of u/D ratio. The depth of first reinforcement beneath the rigid footing was changed as 0.05, 0.10, 0.15, and 0.20 m. Secondly, the effect of vertical spacing between geogrid layers was investigated. Vertical spacing between two reinforcement layers (h) was changed as 0.05, 0.10, and 0.15 m. Table 2 summarizes the testing program and variable parameters u/D and h/D.

3 Results of field tests

3.1 Effect of first geogrid layer reinforcement

The effect of the depth of first geogrid reinforcement within the granular fill layer on bearing capacity behavior

Fig. 2 Schematic view of test setup, loading, and reaction system

Table 2 Details of the field test program

Test series	Constant parameters	Variable parameters	Number of tests done
I	Natural clay	1	
II	$H/D = 0.67$, N = 1	u/D = 0.17, 0.33, 0.50, 0.67	4
III	$H/D = 0.67$, $N = 2$, $u/D = 0.17$	h/D = 0.17, 0.33, 0.50	3

of the footing was investigated in this series. For the tests, the thickness of granular fill layer (H) was kept constant as 0.67D. First geogrid layer depth (u) was changed as 0.05, 0.10, 0.15, and 0.20 m. The bearing capacity keeps increasing with the decrease in the first geogrid layer depth. Figure 3 shows the relationship between bearing capacity (q) and settlement ratio (s/D) for different u values (see also Fig. 2 for the presentation of the parameter, u). Maximum performance on bearing capacity was obtained at $u = 0.05$ m ($u = 0.17D$). At settlement of $s/D = 10$ %, Fig. 3 shows that the bearing capacity increases from 466 kPa (natural clay deposit) to 824 kPa ($u = 0.17D$). It is seen that the placement of geogrid reinforcement within the granular fill layer increases bearing capacity up to 1.8 times. For the same displacement ratio, the inclusion of geogrid layer improves the performance of the footing by increasing the bearing capacity and reducing the settlement. It is shown an improvement in footing performance using geogrid reinforcements, as the transfer of footing loads to greater depths through the geogrid layers and
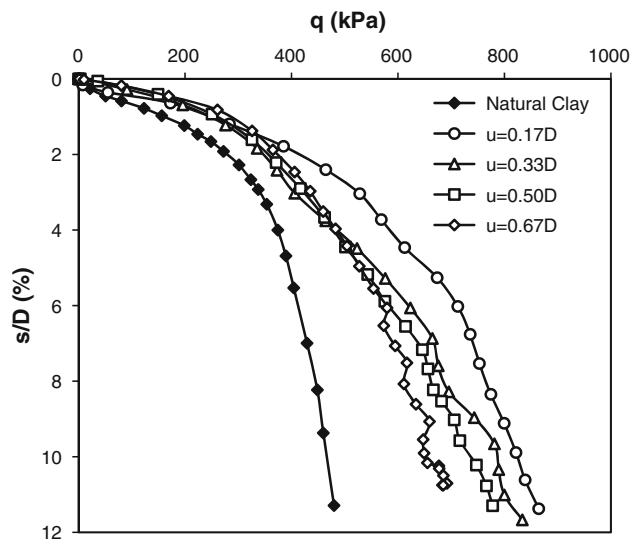
Fig. 3 The effect of depth of single geogrid reinforcement from field tests

interlock between the geogrid and the granular fill reduce lateral and vertical displacements below the footing. The interaction between the geogrid and the fill is dominated by the interlocking of grain particles within the geogrid cells [15, 28]. The purpose of the fill is to provide a suitable operating surface on which concentrated loads may be carried without the subgrade failing or deforming excessively.

3.2 Effect of two-layer geogrid reinforcement

In this series, the influence of the vertical spacing between geogrid layers on the bearing capacity behavior of clay deposits was investigated. For the tests, the values of H and u were kept constant as 0.20 m and 0.05 m, respectively. Vertical geogrid spacing ratio (h/D) is defined as the ratio of vertical spacing between two geogrids (h) to rigid footing diameter (D). The vertical spacing of reinforcement varied from 0.05 m (0.17D) to 0.15 m (0.50D). Figure 4 shows the relationship between bearing capacity (q) and settlement ratio (s/D) for different h values (see also Fig. 2 for the presentation of the parameters, u and h). At settlement of $s/D = 10$ %, the bearing capacities of the reinforced soil increase to 880, 958, and 1,049 kPa, as the vertical spacing between geogrids (h) are 0.17D, 0.33D, and 050D, respectively. It is seen that the placement of second geogrid increases bearing capacity up to 2.25 times. The bearing capacity reaches its maximum value when second geogrid layer was placed at the interface of granular fill and soft clay that h equals to 0.50D.

The effect of geogrid number in bearing capacity is illustrated in Fig. 5. It is shown that increasing the number of geogrid layer from 1 to 2 increases the bearing capacity

of the foundation significantly. The results show a moderate increase in the bearing capacity of a reinforced system at small displacement and a further improvement at large displacement. In particular, stiffness of the reinforced soil increases significantly at large deformations. This is attributed to a tensioned membrane effect in the geosynthetic beneath the footing [18, 27]. Previous studies conducted by other researchers have also shown that increasing the number of reinforcement layers would increase the bearing capacity of reinforced soils [1, 3, 6, 15, 22, 30, 36]. Similar to this observation, the test results presented by Adams and Collin [1] for large square footing on reinforced sand indicated that the benefit increases with an increase in settlement. When reinforcement is present, it prevents the lateral movement of the fill material, so that the base of the fill acts as a fully rough footing on the surface of the clay.

In conventional design, the bearing capacity of a vertically loaded shallow foundation on undrained clay is expressed as:

$$q = N_c c_u \tag{1}$$

where q is the ultimate bearing capacity of the footing and N_c the bearing capacity factor. Normalized load–deformation curves for reinforced and natural clay cases are presented in Fig. 6. The displacement is normalized by D, where D is the diameter of the footing. Bearing capacity values were divided by the undrained cohesion value of c_u (mean value obtained from the field tests is 65 kPa). Maximum value of N_c for natural clay case was found as 6.20 (at $s/D = 12.5$ %) from the field test. The semi-analytical/numerical solution also indicates that, for a circular
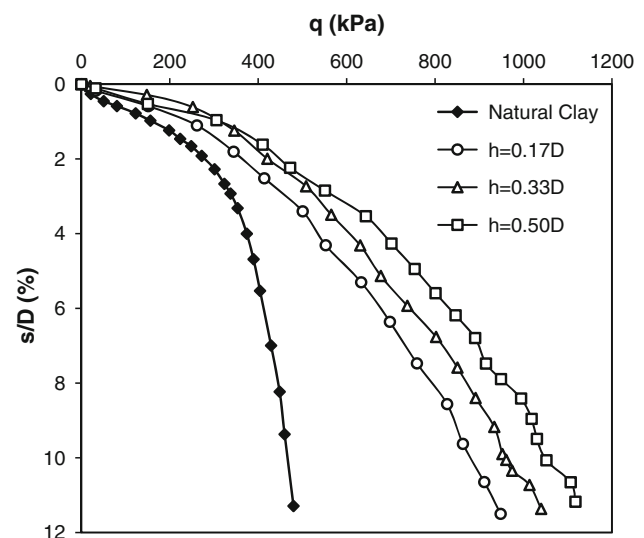

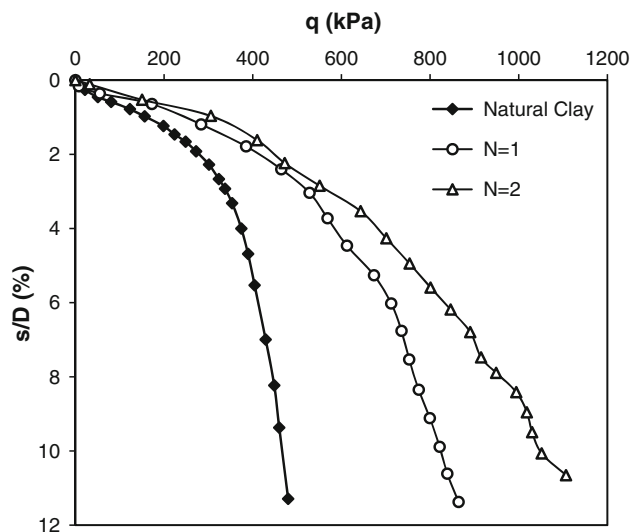**Fig. 4** The effect of vertical spacing between geogrid layers from field tests

Fig. 5 The effect of number of geogrid layers from field tests

Table 3 N_c values for natural clay and reinforced cases

	$N_c = q/c_u$		
	Natural clay	Reinforced ($N = 1$) ($N = 1$, $u = 0.17D$)	Reinforced ($N = 2$) ($N = 2$, $u = 0.17D$, $h = 0.50D$)
s/D (%)			
2	3.6	5.2	5.7
5	4.9	8.1	9.4
10	5.8	10.3	13.2

footing resting on undrained clay with a constant strength, the bearing capacity factor N_c should be 6.20 for rough footing [32]. It is seen in Fig. 6 that N_c increases significantly with an increase in the number of geogrid layers, N. The values of N_c for different s/D ratios are compared in Table 3.

4 Finite element modeling

The FE analyses have been performed to obtain the load–displacement curves for rigid circular footings resting on reinforced and natural clay soil with the same model geometries as in the tests. FE modeling has the advantages that parameters may be easily varied, and details of stresses and deformations throughout the system may be studied. This is particularly valuable for looking at what is happening at the interface between fill and soft clay, which is very difficult to do in a model test. The FE program Plaxis 3D Foundation (Version 2.2) was used in the analyses. The program is a FE package specially developed for the analysis of deformation and stability in geotechnical engineering
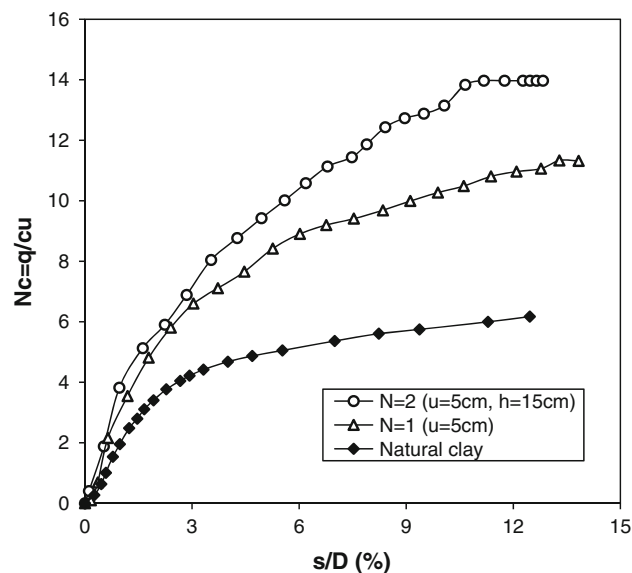

Fig. 6 Normalized load–deformation curve for reinforced and natural clay cases from field tests

problems [4]. A three-dimensional model was adopted to simulate circular footing on reinforced granular fill over clayey soil width and depth equal to 10.0 times the footing diameter (D), respectively. The boundary dimensions for FE analyses were determined by conducting several analyses on different mesh sizes to select the dimension of the mesh in which the footing's bearing capacity is not affected by the boundary conditions. Sensitivity analyses were also conducted to find the degree of mesh refinement to minimize mesh-dependent effects converge on unique solution. Finally, adopted finite element model, which has $10.0D \times 10.0D \times 10.0D$ and includes about 5,000 elements, is illustrated in Fig. 7. The undrained behavior of clay soil was modeled as an elastic-perfectly plastic material with limiting shear stress equal to c_u. The undrained shear strength of clay soil was determined from unconfined compression tests, and undrained elasticity modulus was derived from the plate loading test on the field. Also, fully incompressible behavior is obtained for $v_u = 0.50$. However, taking $v_u = 0.50$ leads to singularity of the stiffness matrix. In order to avoid numerical problems, v_u is taken as 0.35 as suggested by the FE program, PLAXIS. The clay soil model parameters were summarized as undrained shear strength ($c_u = 65$ kPa), undrained elasticity modulus ($E_u = 8,500$ kPa), and Poisson's ratio ($v = 0.35$), respectively. On the other hand, the parameters of granular fill were obtained from conventional laboratory tests. The granular fill was assumed to be a purely frictional granular soil with a friction angle, ϕ' of 43°, and a bulk unit weight, γ of 21 kN/m³. The dilatancy angle ψ was taken as 13° based on the equation proposed by Bolton [5]. The circular footing is modeled as a rigid plate and is considered to be very stiff and rough in the analyses.

Geogrid layers are represented by the use of horizontal plate elements in the program. The plate element is a structural object used to model thin horizontal (two-dimensional) structures in the ground. The stress–strain behavior of geogrid layer was modeled as a linear elastic material. It was assumed to be isotropic, and the basic geometry parameters include the thickness, $d = 0.015$ m, elasticity modulus, $E = 7.33 \times 10^5$ kPa, Poisson's ratio, $v = 0.10$, and the unit weight of the plate material, $\gamma = 0.02$ kN/m^3. The plate element is composed of 6-node triangular plate elements. The reinforcement is treated as perfectly rough, so that any failure must occur in soil elements adjacent to the reinforcement rather than at the interface. Yielding of the reinforcement was not considered, as none was observed in the model tests [27]. However, it is assumed to be fully friction between geogrid and the surrounding soil in the numerical analyses. This means that the friction between geogrids and granular fill is large enough for there to be no relative displacement between the two materials (full friction).

5 Numerical results and discussions

The load–displacement curves obtained from the field test and FE analysis for natural clay and reinforced cases are shown in Fig. 8. In reinforced case, for $N = 1$, the values of H, u were kept constant as 0.20 and 0.05 m; for $N = 2$, the values of H, u, and h were kept constant as 0.20, 0.05, and 0.15 m, respectively. The second reinforced layer was placed at granular fill and clay interface ($h = 0.15$ m). The loading pressure–settlement curves obtained from the tests and the FE analysis show good match for the natural clay case. The predicted responses in reinforced case are
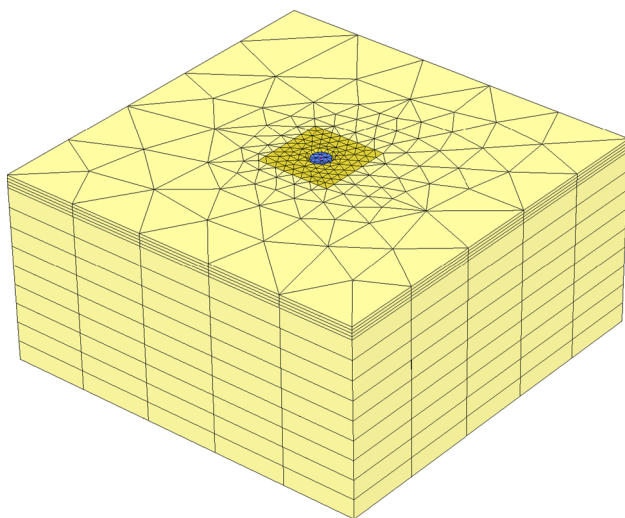
slightly underestimated from the experimental results. The reason for this is that the interlocking effect between soil and reinforcement layer cannot be modeled properly in the numerical analysis. Geogrids have an open grid-like appearance and have been used efficiently to reinforce soil structures. Fill material interacts with a geogrid principally by interlocking within the apertures. The geogrid layer was modeled as a plate without aperture in the analysis.
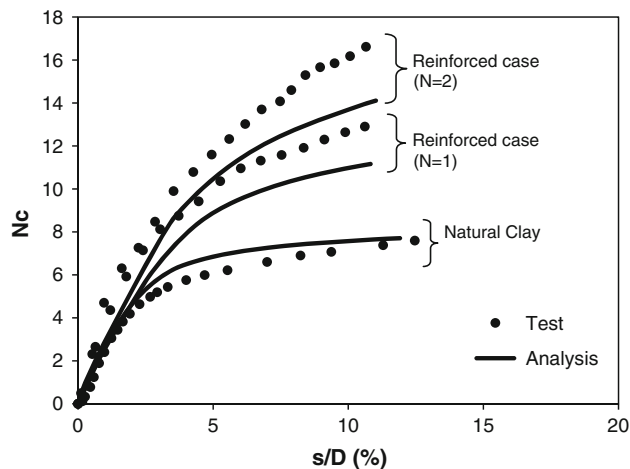

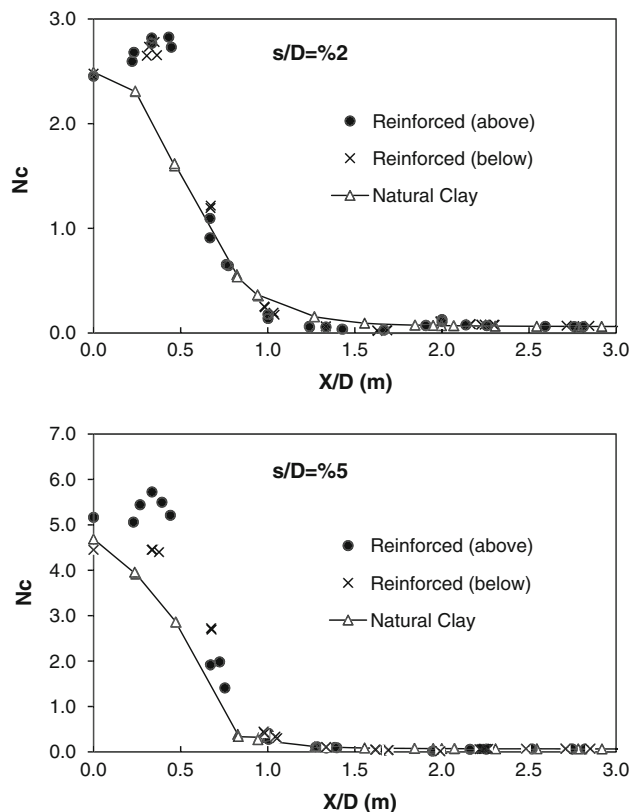Fig. 8 Comparison of finite element predictions with field tests

Fig. 9 Normal stresses at fill/clay interface for reinforced and natural clay cases from numerical analysis

Fig. 7 Typical finite element mesh used in the numerical analyses

However, the results show that such a simple constitutive model can be used in numerical analysis of short time stability of a foundation on soft clay.

Figure 9 shows the calculated normal stress distributions at fill/clay interfaces for natural clay (without fill and reinforcement) and reinforced ($H = 0.20$ m, $N = 2$, $u = 0.05$ m and $h = 0.15$ m) cases. Normal stresses are shown immediately above and below the second reinforcement layer in the reinforced case in Fig. 9. Two different footing penetrations were selected as 2% (initial loading) and 5 % (close to the failure loading) to compare the results. These comparisons provide a better understanding of the reinforcement mechanisms controlling the footing loads in the numerical analyses. As expected, there is a relatively higher pressure in the reinforced case than

that of natural clay case under the footing. The geosynthetic reinforcement at the fill/clay interface is distorted and thus tensioned in high pressure. The predicted reinforcement tension force distributions are shown in Fig. 10. It shows that the maximum tension force developed at the edge of the footing ($X/D = 0.5$) at which the location of maximum shear stress zone ($X/D = 0.5$) and higher tension forces develop on the second reinforcement layer. This shows that the second geogrid layer at the fill/clay interface works more effective at the high footing loads and at the large strains. As pointed out by Love et al. [27], this is due to the combined action of the reinforcement, firstly in containing large outward shear stresses and secondly acting as a membrane.
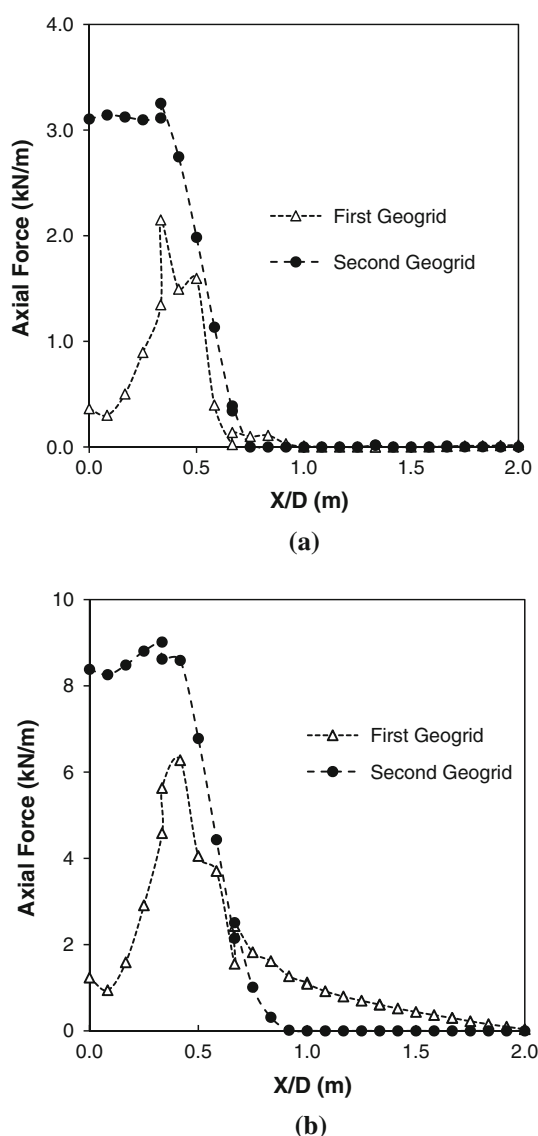

Fig. 10 Axial forces on geogrid layer from numerical analysis. **a** $s/D = 2$ %, **b** $s/D = 5$ %
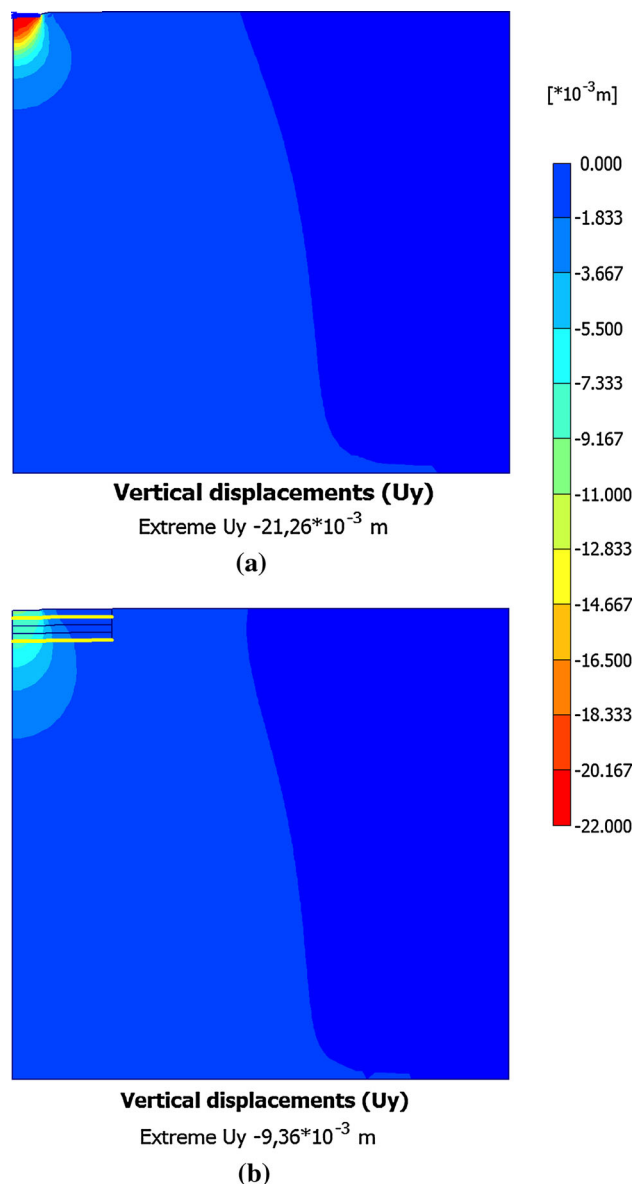

Fig. 11 Vertical displacement fields below the footing. **a** Natural clay, **b** reinforced case ($N = 2$)
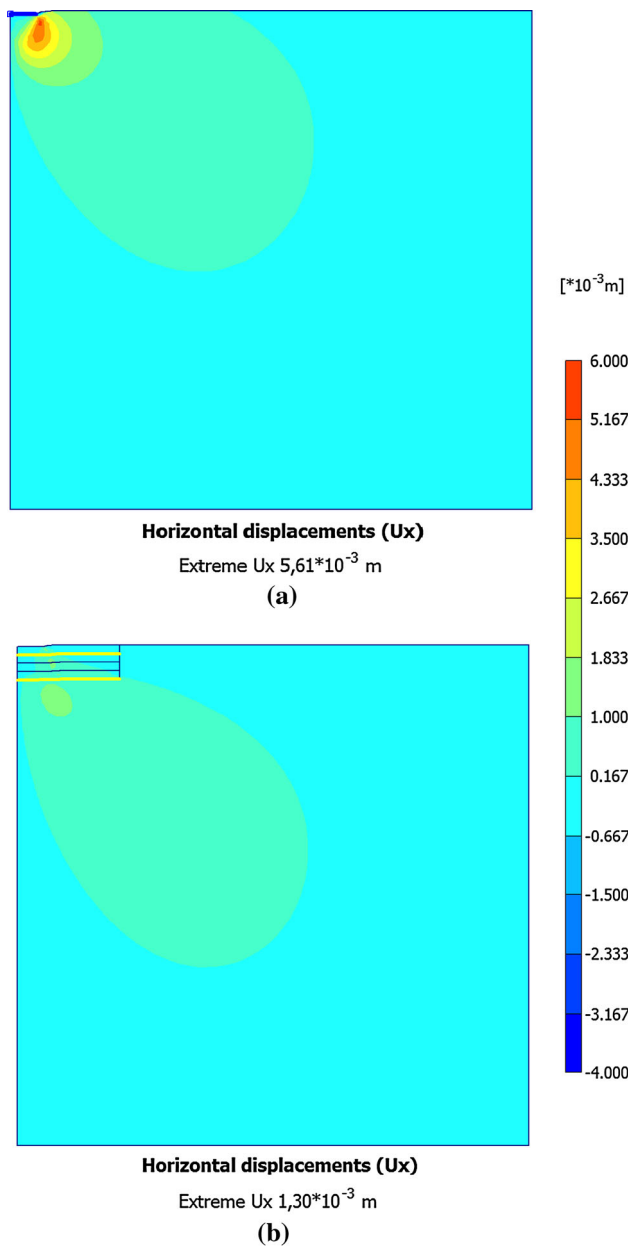
Horizontal displacements (Ux)

Extreme Ux 5,61*10^{-3} m

(a)

Horizontal displacements (Ux)

Extreme Ux 1,30*10^{-3} m

(b)

Fig. 12 Horizontal displacement fields below the footing. **a** Natural clay, **b** reinforced case ($N = 2$)

Fig. 13 Shear stresses at the granular fill–clay interface for reinforced and natural clay cases from numerical analysis. **a** $s/D = 2$ %, **b** $s/D = 5$ %

The numerical analyses show that only when the footing loading approaches to failure, the reinforcement has noticeable effect on vertical and horizontal displacements of the soft clay. Figures 11 and 12 show some typical examples of the resultant vertical and horizontal displacement fields below the footing for natural clay and reinforced cases at a loading pressure which is very close to the failure load of the natural clay subsoil. It can be seen that there is a clear reduction in horizontal and vertical displacements for the reinforced case compared with the natural clay 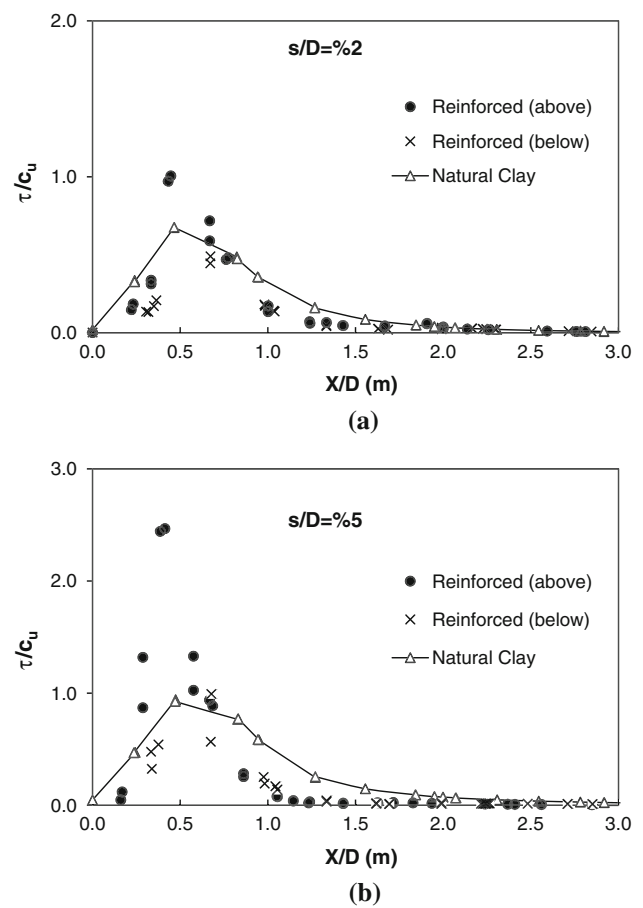case. The reinforced soil structure behaves as a rigid slab below the footing and distributes the load into the underlying ground. This reduces the lateral and vertical displacements, resulting in uniform settlement. Furthermore, interlocking between the geogrid and the fill material prevents lateral and vertical displacements near the footing edge. As seen that the effect of the reinforcement on subsoil deformation can become significant when soft clay approaches to failure. The mobilized tensile force in the reinforcement layers and the confining effect of the reinforcement can increase the bearing capacity and reduce the lateral deformation of soft clay (Fig. 12). In addition, due to its axial stiffness, the curved geosynthetic exerts an upward force supporting the footing load and thus improving the bearing capacity, showing a small membrane effect. The reinforcement layers act like a tensioned membrane, with the pressure on the soft clay being smaller than the pressure applied to the fill on the upper. The reinforcement, while in tension, spreads the load over a larger area, leading to a reduction in the settlement beneath the footing (Fig. 11). Because of confinement effect or lateral restraint effect due to relative displacement between
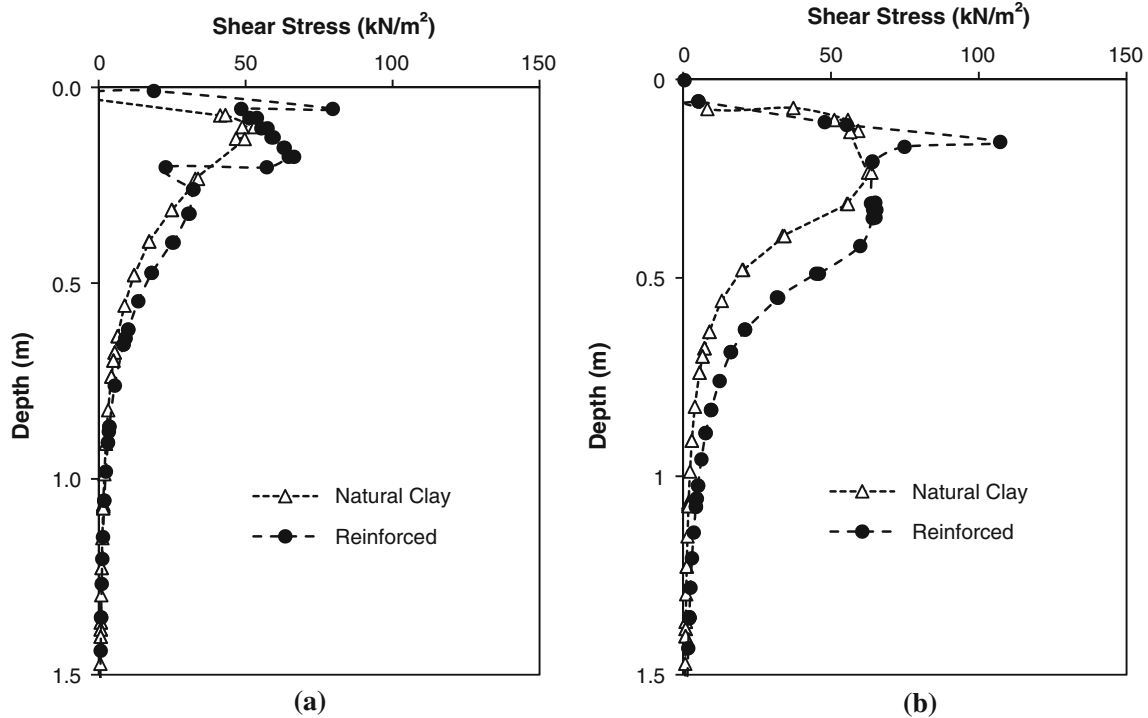
Fig. 14 Change in shear stresses with depth from numerical analysis. **a** $s/D = 2$ %, **b** $s/D = 5$ %
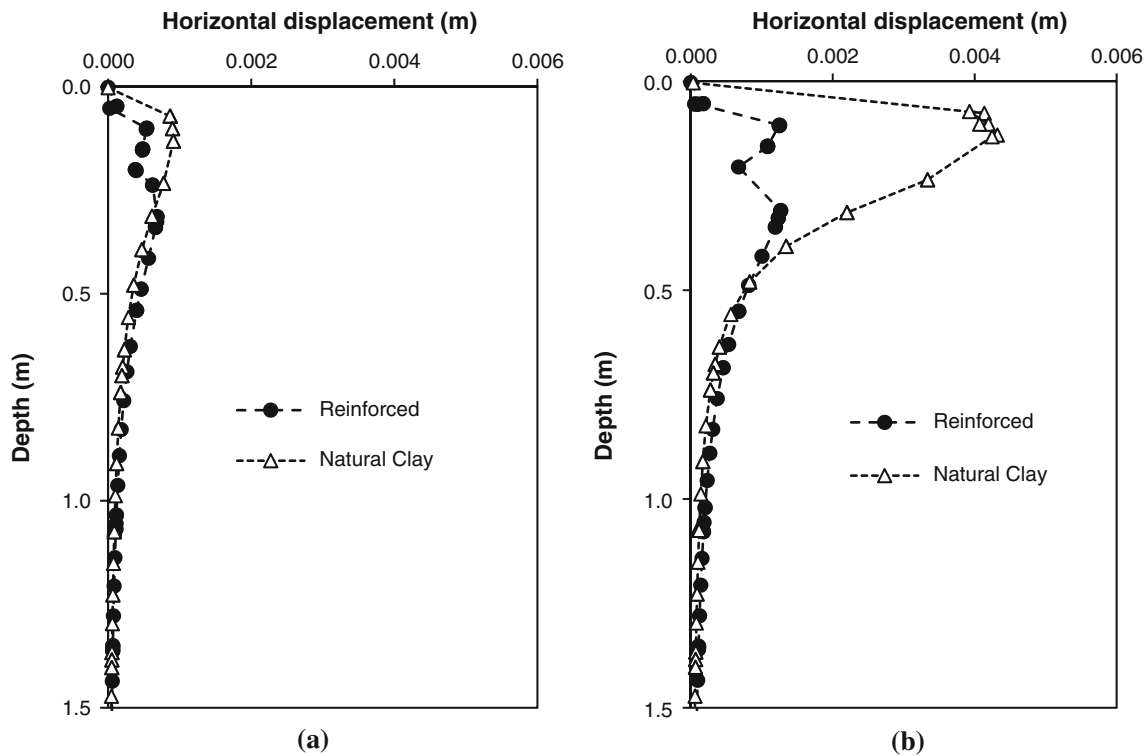
Fig. 15 Change in horizontal displacement with depth from numerical analysis. **a** $q = 300$ kN/m^2, **b** $q = 500$ kN/m^2

soil and reinforcement, the friction force is induced at the soil–reinforcement interface. Furthermore, the interlocking can be developed by the interaction between soil and geogrid. Consequently, lateral deformation or potential tensile strain of the reinforced soil is restrained and vertical displacement of soil is reduced.

Table 4 Typical design parameters for reinforced soil foundations

Parameters			This study		Wayne et. al. [35]		
			Typical value	BCR	Typical value	Recommended value	BCR
H			$0.33D$	1.23	$0.5B$ to $1.0B$	$H < 2.0B$	1.50–2.50
			$0.67D$	1.60			
			$1.00D$	2.04			
$H = 0.33D$	For $N = 1$	u	$0.17D$	1.51	u; $0.15B$ to $0.3B$	$u < 0.5B$	
			$0.33D$	1.46	h; $0.15B$ to $0.3B$	$h < 0.5B$	
	For $N = 2$	$u = h$	$0.17D$	1.78	N; 2–4	$N < 5$	
$H = 0.67D$	For $N = 1$	u	$0.17D$	1.85			
			$0.33D$	1.89			
			$0.50D$	1.88			
			$0.67D$	1.88			
	For $N = 2$	$u = h$	$0.33D$	2.31			
		$u = 0.17D, h = 0.33D$		2.21			
	For $N = 3$	u	$0.33D$	2.50			
		h	$0.17D$				
	For $N = 4$	$u = h$	$0.17D$	2.60			
$H = 1.00D$	For $N = 1$	u	$0.17D$	2.73			
			$0.33D$	2.75			
			$0.50D$	2.67			
			$0.67D$	2.67			
			$0.83D$	2.65			
			$1.00D$	2.30			
	For $N = 2$	$u = h$	$0.17D$	3.13			
		$u = 0.17D, h = 0.67D$		3.17			
	For $N = 3$	$u = h$	$0.17D$	3.31			
	For $N = 4$	$u = h$	$0.17D$	3.41			
	For $N = 5$	$u = h$	$0.17D$	3.54			
	For $N = 6$	$u = h$	$0.17D$	3.71			

D, footing diameter; B, footing width; H, thickness of the granular fill layer; u, depth of first geogrid reinforcement; h, vertical spacing of reinforcement layers; N, number of geogrid layers

Figure 13 shows the shear stress distribution at the fill/clay interface. It is clear that larger shear stresses are occurred in the reinforced case. It can be seen that shear stresses are maximum at the edge of the footing ($X/D = 0.5$). For $s/D = 5$ %, the ratio of τ/c_u is around 2.50 in the reinforced case, while the ratio of τ/c_u is around 1.00 in the natural clay case. As seen that the reinforcement serves to prevent the shear stresses on its upper surface from being transmitted to the clay. In particular, the shear stresses on upper surface of the reinforcement are larger than those below at $s/D = 5$ %. Figures 14 and 15 also show shear stresses and horizontal displacements distribution with depth. Due to frictional interaction and interlocking between the fill material and the geosynthetic, the aggregate particles are restrained at the interface between the clay and the fill. The reinforcement can absorb additional shear stresses between clay and fill, which would otherwise be applied to the soft clay. This significantly improves the load distribution of footing on soft clay. Reinforced granular fill changes the magnitude and orientation of shear stresses on the soft clay in the loaded area. The reinforced granular fill layer also results in redistribution of the applied load to a wider area and thus minimizing stress concentration and achieving improved distribution of induced stress. The redistribution of applied load to a wider area below the reinforced zone leads to an increase in bearing capacity and a decrease in settlement of the foundations compared to the natural clay soil. The construction of wide granular fill layer also leads to "surcharge effect" and can prevent soil from moving upward at locations far away from the rigid footing, and thus improve the bearing capacity of natural clay deposit.

After verification of the numerical analyses, additional extensive parametric studies have been carried out for different thickness of the granular fill layers (H/D of 0.33, 0.67, and 1.00) and reinforcement configurations (u, h, and

N). As seen from the numerical results, the BCR is a function of *H/D*, *u/D*, *h/D*, and *N*. Therefore, numerical results are compared with typical design parameters presented by Wayne et al. [35] based on a comprehensive study of experimental data and literature reviews in Table 4. It shows improvement rates on bearing capacity, and also, the design parameters related to configurations of geogrid reinforcements for practical applications are suggested.

6 Conclusion

The bearing capacity of a circular rigid footing on geogrid-reinforced granular fill layer constructed above natural clay deposits was investigated using 3D FE program Plaxis Foundation and by physical field modeling. Based on this investigation, the following main conclusions can be drawn.

- Numerical analyses, using a simple constitutive model (Mohr–Coulomb model), gave results that closely match those from physical model tests for short-term stability.
- A significant improvement in the bearing capacity of a footing can be obtained by placing a compacted fill layer of limited thickness over soft clay subsoil. The bearing capacity of the footing can be further increased by placing geogrid reinforcement layers within compacted fill layer. Geogrid reinforcement layers within granular fill on soft clay cause to reduce the necessary fill thickness.
- The degree of improvement is related to the thickness of granular fill layer and properties and configuration of geogrid layers. Hence, the design parameters related to configurations of geogrid reinforcements for practical applications should be selected considering thickness of granular fill layer.
- If the thickness of granular fill layer is selected as 0.67*D*, design parameters can be suggested as follow:
- For *N* = 1, the location of the geogrid layer to obtain maximum benefit from the reinforcement should be placed at between 0.10*D* and 0.50*D* below the bottom of the footing. The increase in bearing capacity is about 90 %, and the reduction in settlement amount is 53 %.
- For *N* = 2, the second geogrid layer should be placed at between 0.15*D* and 0.30*D* below the first geogrid layer. The inclusion of second reinforcement increases bearing capacity up to 230 % and decreases settlement up to 60 %.
- The geogrid reinforcement in granular fill increases the stability of the footing by mobilized tensile force in the reinforcement and providing a confinement effect

against lateral shear stress. Reduction in shear stress transmitted from the fill layer to soft clay, which increases the bearing capacity of the soft clay. Geogrid reinforcement also prevents shear failure reducing significantly lateral deformations.
- When comprised to the predicted reinforcement tension force distributions, it is shown that the maximum tension force developed at the edge of the footing (*X/D* = 0.5) at which the location of maximum shear stress zone (*X/D* = 0.5) and higher tension forces develop on the second reinforcement layer.
- The second geogrid reinforcement used at the fill/clay interface; the shear stress distribution at the fill/clay interface shows that larger shear stresses are occurred in the reinforced case. And also, it can be seen that shear stresses are maximum at the edge of the footing (*X/D* = 0.5) for both cases.
- The numerical results show that there is a clear reduction in horizontal and vertical displacements for the reinforced case compared with the natural clay case.

References

1. Adams M, Collin J (1997) Large model spread footing load tests on geosynthetic reinforced soil footings. J Geotech Geoenviron Eng 123(1):66–72
2. ASTM (1997) Standard test method for nonrepetitive static plate load tests of soils and flexible pavement components, for use in evaluation and design of airport and highway pavements, pp 112–113
3. Binquet J, Lee KL (1975) Bearing capacity tests on reinforced earth slabs. J Geotech Eng Div ASCE 101(GT12):1241–1255
4. Brinkgreve RBJ, Vermeer PA (1998) Finite element code for soil and rock analyses. A. A. Balkema, Rotterdam
5. Bolton MD (1986) The strength and dilatancy of sands. Geotechnique 36(1):65–78
6. Chen Q (2007) An experimental study on characteristics and behavior of reinforced soil footing. PhD Thesis, Louisiana State University, Baton Rouge, USA
7. Consoli NC, Schnaid F, Milititsky J (1998) Interpretation of plate load tests on residual soil site. J Geotech Geoenviron Eng 124(9):857–867
8. DeMerchant MR, Valsangkar AJ, Schriver AB (2002) Plate load tests on geogrid reinforced expanded shale lightweight aggregate. Geotext Geomembr 20:173–190
9. Fannin RJ, Sigurdsson O (1996) Field observations on stabilization of unpaved roads with geosynthetics. J Geotech Eng 122(7):544–553
10. Fonseca V (2001) Load tests on residual soil and settlement prediction on shallow footing. J Geotech Geoenviron En 127(10):869–883
11. Gabr MA, Hart JH (2000) Elastic modulus of geogrid reinforced sand using plate load tests. Geotech Test J 23(2):245–250

12. Giroud JP, Noiray L (1981) Geotextile-reinforced unpaved road design. ASCE J Geotech Eng Div 107(GT9):1233–1254
13. Giroud JP, Ah-Line C, Bonaparte R (1984) Design of unpaved roads and traffic areas with geogrids. In: Symposium on polimer grid reinforcement. Institution of Civil Engineers, London
14. Hirofumi F, Jun'ichi N, Koichi T (2003) A Study on the scale effect of ultimate bearing capacity on rock fill. Mon Rep Civil Eng Res Inst 600:21–28
15. Huang CC, Tatsuoka F (1990) Bearing capacity reinforced horizontal sandy ground. Geotext Geomembr 9:51–82
16. Hufenus R, Rueegger R, Banjac R, Mayor P, Springman SM, Brönnimann R (2006) Full-scale field tests on geosynthetic reinforced unpaved roads on soft subgrade. Geotext Geomembr 24:21–37
17. Khing KH, Das BM, Puri VK, Cook EE, Yen SC (1993) The bearing capacity of a strip footing on geogrid reinforced sand. Geotext Geomembr 12:351–361
18. Kinney TC (1979) Fabric induced changes in high deformation soilfabric-aggregate systems. PhD thesis, University of Illinois at Urbana, Champaign, Ill
19. Laman M, Yildiz A (2003) Model studies of ring foundations on geogrid-reinforced sand. Geosynth Int 10(5):142–152
20. Laman M, Yildiz A, Demir A, Ornek M (2008) Shallow foundations on geogrid reinforced soft clay. In: 4th European geosynthetics conference (EuroGeo4), Edinburgh, Scotland, 7–10 September
21. Laman M, Yildiz A, Ornek M, Demir A (2009) Geogrid reinforcement on soft clay deposit. TUBITAK Scientific Research Project (No:106M496), Ankara, Turkey, 528 p
22. Laman M, Yildiz A, Ornek M, Demir A (2010) Experimental and numerical analysis of circular foundations rested on geogrid reinforced clay soils. In: 9th International conference on geosynthetics Sofitel Jequitimar, Guarujá, SP, Brazil
23. Laman M, Yildiz A, Ornek M, Demir A (2012) Field test of circular footing on reinforced granular fill layer overlying clay bed. Geotech Test J 35(4). doi:10.1520/GTJ103512
24. Ling HI, Liu Z (2001) Performance of geosynthetic reinforced asphalt pavements. J Geotech Geoenviron Eng 127(2):177–184
25. Ling HI, Liu H (2003) Finite element studies of asphalt concrete pavement reinforced with geogrid. J Eng Mech ASCE 129(7):801–811
26. Ling HI, Liu H (2009) Deformation analysis of reinforced soil retaining walls—simplistic versus sophisticated finite element analyses. Acta Geotech 4(3):203–213
27. Love JP, Burd HJ, Milligan GWE, Houlsby GT (1987) Analytical and model studies of reinforcement of a layer of granular fill on a soft clay subgrade. Can Geotech J 24(4):611–622
28. Michalowski RL (2004) Limit Loads on reinforced foundation soils. J Geotech Geoenviron Eng ASCE 130(4):381–390
29. Miura N, Sakai A, Taesiri Y, Yamanouchi T, Yasuhara K (1990) Polymer grid reinforced pavement on soft clay ground. Geotext Geomembr 9(1):99–123
30. Omar MT, Das BM, Yen SC, Puri VK, Cook EE (1993) Ultimate bearing capacity of rectangular footings on geogrid-reinforced sand. Geotech Test J ASTM 16(2):246–252
31. Ornek M (2009) Geogrid reinforcement on soft clay deposits. PhD Thesis, University of Cukurova, Turkey, 318 p (in Turkish)
32. Potts DM, Zdravkovic L (2001) Finite element analysis in geotechnical engineering: application. Thomas Telford, London
33. Rowe RK, Soderman KL (1986) Reinforced embankments on very poor foundations. Int J Geotext Geomembr 4(1):65–81
34. Rowe RK, Li LL (2005) Geosynthetic—reinforced embankments over soft foundations. Geosynthetics International, Special Issue on the Giroud Lectures 12(1):50–85
35. Wayne MH, Han J, Akins K (1998) The design of geosynthetic reinforced foundations. In: Bowders JJ, Scranton HB, Broderick GP (eds) Geosynthetics in foundation reinforcement and erosion control systems, Geotechnical special publication no. 76, pp 1–18
36. Yetimoglu T, Wu JTH, Saglamer A (1994) Bearing capacity of rectangular footings on geogrid-reinforced sand. J Geotech Eng ASCE 120(12):2083–2099
37. Yamamoto K, Lyamin AV, Abbo AJ, Sloan SW, Hira M (2009) Bearing capacity and failure mechanism of different types of foundations on sand. Soils Found 49(2):305–314